

		 National Oceanography Centre NATURAL ENVIRONMENT RESEARCH COUNCIL	
			
		 ALONG-TRACK	 Consiglio Nazionale delle Ricerche
			

# HYDROCOASTAL

## SAR/SARin Radar Altimetry for Coastal Zone and Inland Water Level

### *Product Validation Plan*

### Deliverable D2.4

Sentinel-3 and Cryosat SAR/SARin Radar Altimetry for Coastal Zone and Inland Water

ESA Contract 4000129872/20/I-DT

Project reference: HYDROCOASTAL\_ESA\_PVP\_D2.4

Issue: 2.0

22/09/2020

This page has been intentionally left blank

## Change Record

Date	Issue	Section	Page	Comment
24/07/2020	1.0			First version
22/09/2020	2.0	various	various	Updates following ESA review. Addition of section 3.7.

## Control Document

Process	Name	Date
Written by:	Mathilde Cancet, Luciana Fenoglio-Marc, Christine Gommenginger, Jesús Gómez-Enri, Andrew Shaw, Denise Dettmering, Pierre Fabry, Nicolas Bercher, Karina Nielsen, Elena Zakharova, Joana Fernandes, Angelica Tarpanelli	22/09/2020
Checked by	David Cotton	
Approved by:		

Subject	Radar Altimetry for Coastal Zone and Inland Water Level	Project	HYDROCOASTAL
Author	Organisation	Internal references	
Mathilde Cancet	NOVELTIS	HYDROCOASTAL_ESA_PVP_D2.4	
Luciana Fenoglio-Marc	U Bonn		
Christine Gommenginger	NOC		
Jesus Gómez-Enri	U Cadiz		
Andrew Shaw	Skymat		
Denise Dettmering	TUM		
Pierre Fabry	Along Track		
Nicolas Bercher	AltHydroLab		
Karina Nielsen	DTU		

Elena Zakharova	NUIM	
Joana Fernandes	U Porto	
Angelica Tarpanelli	CNR-IRPI	

	Signature	Date
For HYDROCOASTAL team		
For ESA		

# Table of Contents

<b>TABLE OF CONTENTS</b> .....	<b>5</b>
<b>1 INTRODUCTION</b> .....	<b>6</b>
1.1 The HYDROCOASTAL Project.....	6
1.2 Scope of this Report.....	6
1.3 Document Organisation .....	6
1.4 Reference documents .....	6
<b>2 VALIDATION OF THE TEST DATASETS IN DIFFERENT COASTAL ZONE SCENARIOS</b> .....	<b>7</b>
2.1 Validation in the German Bight/Baltic Sea region (U Bonn).....	7
2.1.1 Times series of data.....	8
2.1.2 Data screening.....	9
2.1.3 Validation approaches .....	9
2.2 Validation in the Harvest region (NOC).....	12
2.3 Validation in the Gulf of Cadiz and Strait of Gibraltar regions (U Cadiz).....	15
2.3.1 Study areas.....	15
2.3.2 Times series of data.....	17
2.3.3 Data screening.....	18
2.3.4 Statistical approaches.....	18
2.4 Influence of land proximity and angle of approach (SatOC/SKYMAT).....	19
<b>3 VALIDATION OF THE TEST DATASETS IN DIFFERENT INLAND WATER SCENARIOS</b> .....	<b>21</b>
3.1 Validation on the Rhine and Elbe rivers (U Bonn).....	21
3.2 Validation of Water Level Time Series (DGFI/TUM) .....	22
3.3 WFRWF approach, influence of ground-track orientation and water fraction (ATK) .....	23
3.4 Validation over the Amazon Basin (AHL).....	24
3.5 Validation against in situ data for Amur, Yangtze and Zambezi (DTU).....	25
3.6 Validation against in situ data for Ob and Rhine Rivers (NUIM) .....	29
3.7 Validation against in situ data for Po and Mississippi Rivers (CNR-IRPI).....	30
<b>4 VALIDATION OF NEW DTC AND WTC OVER CZ AND IW REGIONS (UPORTO)</b> .....	<b>32</b>
4.1 Validation of the WTC .....	32
4.2 Validation of the DTC .....	32
<b>5 REFERENCES</b> .....	<b>33</b>
<b>LIST OF ACRONYMS</b> .....	<b>37</b>

# 1 Introduction

## 1.1 The HYDROCOASTAL Project

The HYDROCOASTAL project is a project funded under the ESA EO Science for Society Programme, and aims to maximise the exploitation of SAR and SARin altimeter measurements in the coastal zone and inland waters, by evaluating and implementing new approaches to process SAR and SARin data from CryoSat-2, and SAR altimeter data from Sentinel-3A and Sentinel-3B.

One of the key objectives is to link together and better understand the interactions processes between river discharge and coastal sea level. Key outputs are global coastal zone and river discharge data sets, and assessments of these products in terms of their scientific impact.

## 1.2 Scope of this Report

This document is the Product Validation Plan (PVP) report for HYDROCOASTAL and it corresponds to the deliverable D2.4. of the project. The scope of this report is to describe the validation activities that will be carried out during the project.

## 1.3 Document Organisation

This document is organised in four main sections:

- Section 1: A short introduction defining the scope of this report.
- Section 2: The activities planned to validate the L2 products in the coastal zones (CZ).
- Section 3: The activities planned to validate the L2, L3 and L4 products in the inland waters (IW).
- Section 4: The validation activities for the new Wet and Dry Troposphere corrections.

## 1.4 Reference documents

HYDROCOASTAL Proposal: SAR/SARin Radar Altimetry for Coastal Zone and Inland Water Level. Proposal, January 2020.

## 2 Validation of the Test Datasets in different Coastal Zone Scenarios

In this section, we describe the activities that will be carried out to validate the Test Dataset Geophysical parameters against other satellites and in situ data, in different Coastal Zone Scenarios (e.g. low lands, cliffs, fjords, cays, estuaries and man-made structures).

These validation activities include the analysis of the influence of land proximity and ground-track orientation on SAR/SARin, analyses and exploitation of SAR/SARin stack data, the analyses of the different algorithms proposed to produce the final dataset and validation against independent observations.

### 2.1 Validation in the German Bight/Baltic Sea region (U Bonn)

The validation activities focus on the German Bight and Baltic Sea coastal region and include the Elbe estuary. The goal is to carry out a characterization of the product performance with estimation of the data accuracy. U Bonn will perform a cross-validation analysis of the new SAR products against other altimeter products, model data and in-situ data. The study area has been used for the validation of radar altimeter data in open ocean and near the shore, see Fenoglio et al. (2015, 2019, 2020) and Dinardo et al. (2018, 2020).

The German Bight region is a mesotidal environment with varying geometry and difficult-to-couple interactions between the meteo-oceanographic and morphodynamical factors. A major similarity among the Elbe, Ems and Weser estuaries is the tidal and atmospheric forcing. Semidiurnal tides with a range of ~3–4m during spring periods are the major drivers. The tidal wave propagates up to the weirs, which are in Herbrum for the Ems, Bremen-Hemelingen for the Weser and Geesthacht for the Elbe. The distances from the mouths to the limnic parts of the estuaries are comparable: from ~30–40 km in the estuaries of Ems and Weser to ~70 km in the Elbe Estuary. The long-term river runoff of Ems, Weser and Elbe is ~80, 330, and 710 m<sup>3</sup>/s, respectively. On the contrary, in the Baltic Sea the ocean tidal signal is very small.

A large network of fiducial reference measurements and model data are available through the German national agencies (BfG, BKG, and BSH). The water level data are from the German Federal Institute of Hydrology (BfG) database (<https://www.pegelonline.wsv.de>) and from BSH. Most stations are co-located with a GPS station and the ellipsoidal height of the zero marker of the tide gauge data are made available by BfG and by the Federal Agency for Cartography and Geodesy (BKG). The height of the zero marker is known for all stations above the national reference height system (NHN). The PSMSL and SONEL databases include some of them (TGBF, TGCU, TGWD, WARN, SASS and TGKI). Sixteen stations have been used to study sea level change from conventional and SAR altimetry in Fenoglio et al. (2020) and along-track SAR data were found to give rmse between 2 cm and few decimeters compared to in-situ data. The tide gauge stations available for this study (triangle) are shown together with wave station data available from BSH (square) in Fig. 2.1.1.

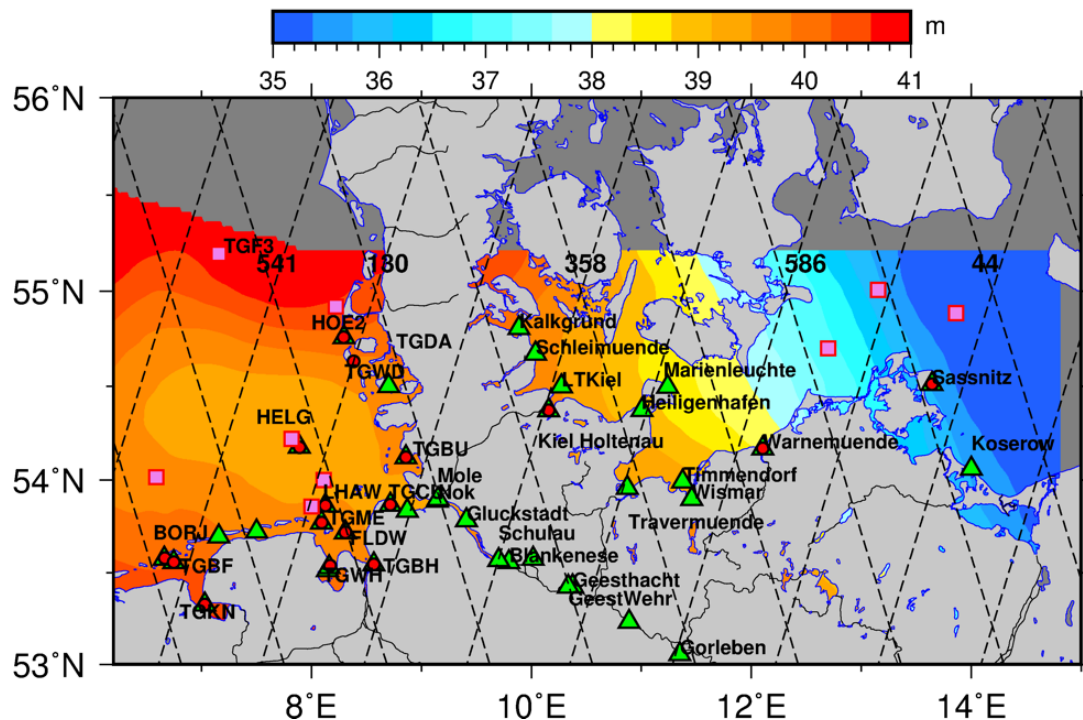


Figure 2.1.1. Region selected and in-situ data. Stations with water level (green triangle), GPS (red circle) and wave height measurements (pink square).

### 2.1.1 Times series of data

The altimetry-derived sea level heights above the ellipsoid WGS84 (SSH<sub>i</sub>) are obtained by applying all the environmental and selected geophysical corrections depending on the application. For the in-situ and model validation, the ocean tide correction and the Dynamic Atmospheric Correction (DAC) are not applied. The Range is corrected for the effect of ionosphere, wet and dry troposphere (Range Corrections in Eq. 2.1.1) and for the solid earth tide, load tide and for the part of the pole tide related to the solid earth (Geophysical Corrections<sub>i</sub> in Eq. 2.1.1 below, see also Eq. 3-5 in Fenoglio-Marc et al., 2015). The sea state bias correction applied is 4.7 % of the significant wave height. The solid earth tide correction does not include the zero-frequency term, called permanent tide, thus the altimeter heights are referred to the mean tide system.

The HYDROCOASTAL altimeter-derived SSH<sub>i</sub> instantaneous time series to be compared to the uncorrected tide gauge observations will be calculated using Eq. (2.1.1):

$$\text{SSH}_i = \text{Altitude} - \text{Range} - (\text{Range Corrections} + \text{Geophysical Corrections}_i) \quad (2.1.1)$$

with Range Corrections including all the environmental corrections and Geophysical Corrections<sub>i</sub> including all the geophysical corrections except the Dynamical Atmospheric Correction (DAC) and the ocean tide.

The TG time series will be built using the time of the closest measurements to the time of the altimeter data. The time sampling of TG data is 1 min for coastal and open sea stations, in case of gaps at the station the time lag accepted between altimetry and tide gauge data is 5 minutes. The Sea Level Height of the TG in the mean height system will be obtained from Eq. (2.1.2)

$$\text{SSH}_{i\_TG} = \text{Water Level} + \text{TG}_{\text{zero}} \quad (2.1.2)$$

with *Water Level* the tide gauge measurement and  $\text{TG}_{\text{zero}}$  the ellipsoidal height in the mean tide system of the reference point (zero) of the tide gauge zero. Eq. (2.1.1) and (2.1.2) allow an absolute comparison of heights, which is possible only when the GPS (red circle in Figure 2.1.1) and the tide gauge (green triangle) are co-located. If  $\text{TG}_{\text{zero}}$  is not available from GPS, the comparison of the sea level anomalies ( $\text{SLA}_i$ ) is made considering the height anomalies of SSHi over a given time interval, which corresponds to the subtraction of a mean sea surface MSS (see Eq. 2.1.3).

$$\text{SLA}_i = \text{Altitude} - \text{Range} - (\text{Range Corrections} + \text{Geophysical Corrections}_i) - \text{MSS} \quad (2.1.3)$$

$$\text{SLA}_{i\_TG} = \text{Water Level} - \text{mean}(\text{Water Level}) \quad (2.1.4)$$

A large part of the residual differences between  $\text{SLA}_i$  and  $\text{SLA}_{i\_TG}$  arises from the difference in ocean tide at the two locations. The residuals are further reduced by applying the ocean tide correction estimated by an ocean model at each location using Eqs. (2.1.5) and (2.1.6) to compute the time series.

$$\text{SLA} = \text{Altitude} - \text{Range} - (\text{Range Corrections} + \text{Geophysical Corrections}_i) - \text{MSS} - \text{ocean tide} \quad (2.1.5)$$

$$\text{SLA}_{TG} = \text{Water Level} - \text{mean}(\text{Water Level}) - \text{ocean tide} \quad (2.1.6)$$

The two last equations are similar, but not coincident, to Eqs. (2.3.1) and (2.3.2). The difference lies in the corrections applied (pole tide related to the solid earth, no DAC, ocean tide from model at the tide gauge in Eqs. 2.1.3 and 2.1.4)

The time sampling of wave data (square in Fig. 2.1.1) is 10 minutes, in case of gaps at the station the time lag accepted between altimetry and wave data is 30 minutes.

### 2.1.2 Data screening

A first screening of the altimeter data consists of rejecting data over land, inland waters and shallow water depth lower than 2 m. Secondly, we apply thresholds to SSH and SWH eliminating SSH data with departure from the mean sea surface (MSS) larger than 15 m and SWH outside the range between -1.5 m and 15 m. Thirdly, different outlier detection rules are applied to the sea level anomaly (SLA) and SWH parameters in coastal and in open sea separately. Standard outlier detection rule is a 3-sigma criterion, moreover the measurements are filtered using the misfit parameter between the model and data waveforms if available for the given retracker. A high value of misfit indicates land contamination or a waveform corresponding to a specular surface. As the SLA in the coastal zone is normally distributed and the SWH is not, the misfit criterion is preferable for the SWH parameter (Dinardo et al., 2018).

### 2.1.3 Validation approaches

An along-track comparison of the data with computation of the statistics (bias, standard deviation of differences and correlation) over a selected part of the track are evaluated (Figure 2.1.2). The new SAR products will be cross-validated against other new and standard products and against ocean model data in scatterplots in open sea and coastal areas. See Figure 2.1.3 for an example of scatterplot comparing Sentinel-3A 1 Hz sea level anomalies in open sea from SAMOSA+ and SAMOSA2 (Dinardo et al., 2020). The average in bands of 200 meters of the standard deviation of sea level anomalies (STD<sub>SLA</sub>) as a function of the distance to the coast will be analyzed for altimetric products and models. One model is taken as reference and the departure between the altimeter and this model is assumed to indicate land contamination in the altimeter data.

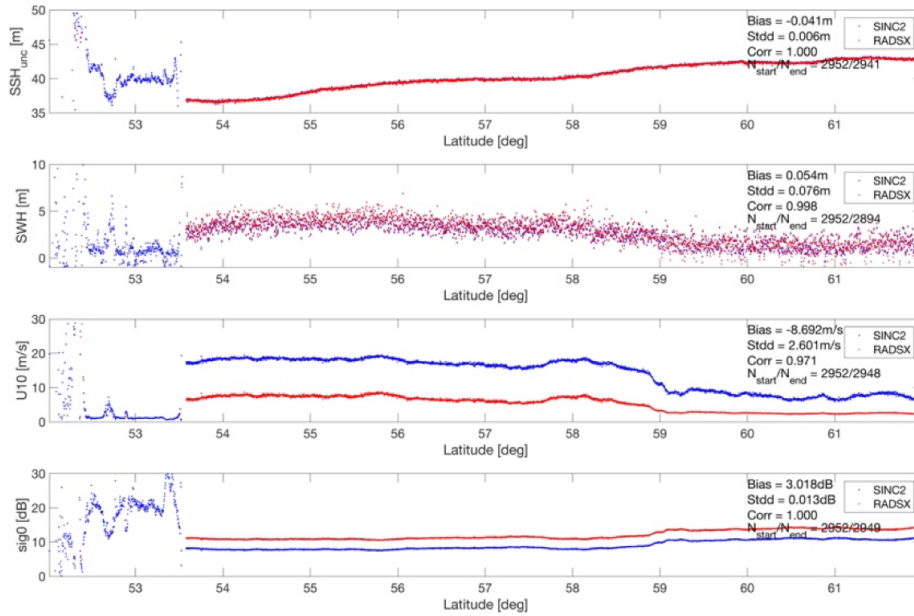


Figure 2.1.2. Along-track comparison of the CryoSat-2 geophysical parameters from different products. In this case Pseudo LRM from the RADSX database (20Hz RADS-Brown retracker, R.Scharroo personal communication) and TUDaBo database (20 Hz SINC2 retracker, Buchhaupt e al., 2018).

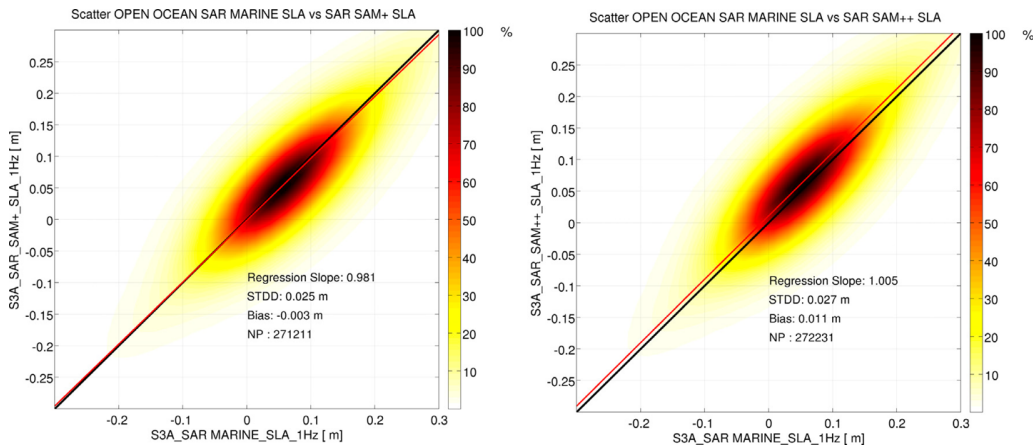


Figure 2.1.3. Scatterplots of Sentinel-3A 1 Hz sea level anomalies in open sea from SAMOSA+ and SAMOSA2 (Dinardo et al., 2020).

To investigate the precision of each single product separately, we investigate the standard deviation of SLA as a function of the SWH. An example is shown in Figure 2.1.4 for the SAR Marine and SAR SARvatore SAMOSA++ products (Dinardo et al., 2020). The quality of the altimeter data is investigated in terms of noise level, with the noise estimated as the absolute value difference between consecutive SSH measurements at 20 Hz. An example is shown in Figure 2.1.5 for the SAR SARvatore SAMOSA+ and the RDSAR TUDaBo products (Fenoglio et al., 2020). The nearest measurements at 1 Hz and 20 Hz within a selected range of distances from the tide gauge stations are selected and time-series are built. The statistics (bias, standard deviation of differences (STDD)) is computed from the two time-series.

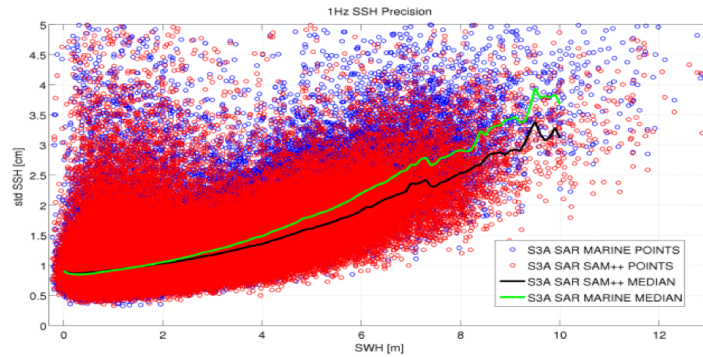


Figure 2.1.4. Standard deviation of SLA as a function of the SWH for the SAR MarineSAMOSA2 and SAR SARvatore SAMOSA++ products

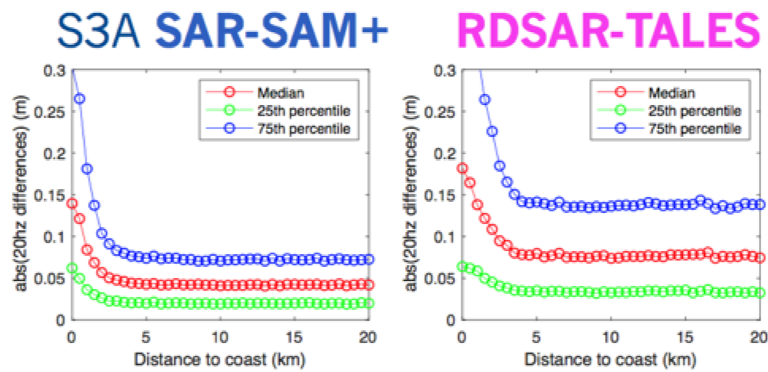


Figure 2.1.5. Noise level of the SSH measurements at 20 Hz for the SAR SARvatore SAMOSA+ and the RDSAR TUDaBo products

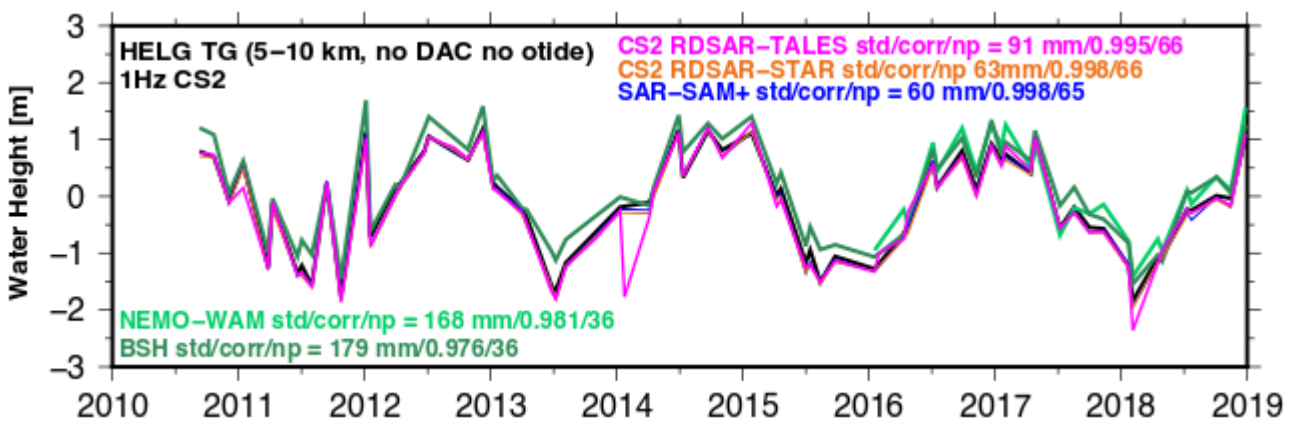


Figure 2.1.6. Sea level anomalies of CryoSat-2 at tide gauge Helgoland uncorrected for ocean tide and DAC.

## 2.2 Validation in the Harvest region (NOC)

The validation activities will focus on the Harvest region on the West coast of the United States.

The region is of interest for validation because of the large number of high-quality in situ measurements of sea level, wave height and wind speed from tide gauges and moored wave buoys in the region. Data from large network of fiducial reference measurements are available freely through the Global Sea Level Observing System (GLOSS) tide gauge network (available via the University of Hawaii Sea Level Centre, UHSLC; <https://uhslc.soest.hawaii.edu/>), and the US National Data Buoy Center (NDBC; [www.ndbc.noaa.gov](http://www.ndbc.noaa.gov)). The GPS data will be obtained from SONEL (<https://www.sonel.org>).

In addition, the region offers several other characteristics that make this a particularly interesting and challenging site to test innovative algorithms for coastal SAR processing such as NOC's Specialised COastal OPERator for SAR waveforms (SCOOP-SAR):

- the west-facing Pacific coastline is famously subject to energetic swell and high sea states in winter, providing a wide range of conditions in a relatively short period (1 year minimum). The dense (relatively) network of wave buoys provide in situ measurements of the full set of wind and sea state parameters (e.g., wave period, and in some cases, directional wave spectra) to support validation of retrieved sea state both offshore and inshore.
- the general orientation of the coastline (SE-NW) offers a variety of oblique approaches to the satellite tracks
- the nature of the coastal land mass (coastal mountains, urban areas, inland water) present many opportunities for contamination of ocean echoes from inland targets.
- the presence of a string of coastal islands.

Figure 2.2.1 shows the area where satellite data will be acquired and processed, the location of in situ stations, the Cryosat-2 SAR mode acquisition box and the ground-tracks of the Sentinel-3A and 3B altimeters.

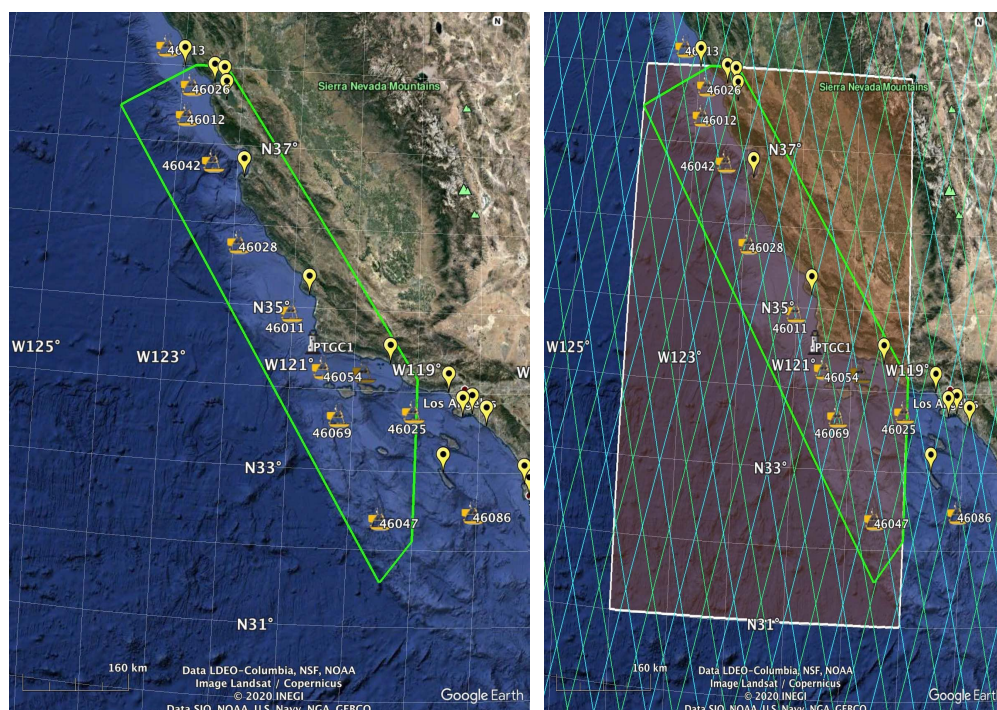


Figure 2.2.1. (left) Harvest validation test site (green polygon) showing the location of coastal tide gauges (yellow/black markers) and moored wind and wave buoys. (right) Same with Cryosat-2 Harvest SAR mode box and Sentinel-3A/B STM ground tracks (blue/green lines).

### 2.2.1 Assessing improvements in data recovery and quality

Improving the recovery and quality of SAR altimeter data close to land is the main objective of advanced coastal SAR retracers. The new coastal SAR datasets will be evaluated using standard diagnostic tools used in coastal altimetry. These will be applied to sea surface height (and derivative products, e.g. SSHA) and significant wave height. Assessment of wind speed will be attempted but may raise issues linked to the dependence of  $\sigma_0$  on wind speed close to land. The coastal altimetry assessment metrics and diagnostic tools to be used include:

- % valid data recovery with distance to coast
- Median/Std with distance to coast
- Misfit
- Std v significant wave height

The assessment will NOT include power density spectra (e.g. of SSH or SWH) since those may not provide reliable results over such a small region.

### 2.2.2 Validation against in-situ data

The SAR altimeter measurements of SSH, SWH and wind speed will be validated against in situ data.

Validation of SAR altimeter wind and wave data will use standard match-up methods with moored buoy data from available NDBC stations. NDBC wind and wave data are 20-minute averages reported hourly or half-hourly. Maximum separation time between the altimeter and in situ wind and wave data will thus be 30

minutes, nominally. In the case of SWH, we will remove values larger than 15 m. Note that the validation of SAR wind speed will only be tentative given the added complexity of validating coastal winds.

In the case of SSH, the validation will be conducted against tide gauges. Comparisons will be done in terms of absolute heights (i.e., ellipsoidal heights) wherever there is a geodetic tie between the TG and a nearby GPS station, otherwise the comparison will be based on sea level anomalies (SLAs).

The altimetric SSHs will be computed by subtracting the corrected range from the altitude, where the former is defined as the range corrected for ionospheric and tropospheric (wet and dry) path delays as well as sea state bias (SSB). The corrections across regions and algorithms will be harmonized to facilitate comparisons with other algorithms and other regions (i.e. German Bight/Baltic and Cadiz/Gibraltar).

In designing a validation strategy for SSH, it is important to recognize that generally altimetry measurements are not collocated with the tide gauges. This spatial separation will necessarily lead to differences in sea levels between the two types of measurements, and the ocean tide can be a major contributor to such differences. Hence, here the comparison will be conducted for detided time series, noting that while tide gauges only sense the ocean tide and the ocean pole tide, altimeter measurements are also influenced by the solid earth tide, the load tide, and the solid earth pole tide, and so these tidal contributions will all be removed from the altimetry data. With this in mind, the altimetric SSHs will be computed according to:

$$\text{SSH} = \text{Altitude} - \text{Corrected\_Range} - \text{Geophysical\_Corrections} \quad (2.2.1)$$

where Geophysical\_Corrections denote the solid earth, pole, load, and ocean tides. Note that we do not apply the DAC.

The SLAs are computed by subtracting the mean sea surface (MSS) from the SSHs:

$$\text{SLA} = \text{SSH} - \text{MSS} \quad (2.2.2)$$

As part of the screening of the altimetry data, we will remove values of SLAs (in both the SSH and the SLA) beyond 2 m and beyond 3 standard deviations.

The relative sea levels from the tide gauges are expressed with respect to the ellipsoid using the following equation:

$$\text{SSH\_TG} = \text{Water\_Level} + \text{TG}_{\text{zero}} - \text{Ocean\_Tide} - (\text{MSS}_{\text{TG}} - \text{MSS}) \quad (2.2.3)$$

where Water\_Level is the relative sea level as observed by the tide gauge,  $\text{TG}_{\text{zero}}$  is the ellipsoidal height in the mean tide system of the reference point of the tide gauge zero, Ocean\_Tide denotes the ocean tide (including the ocean pole tide), and  $\text{MSS}_{\text{TG}}$  is the mean sea surface at the TG location. The term within parenthesis on the right-hand side of Eq. (2.2.3) accounts for differences in the mean sea surface due to spatial separation between the altimetry and the tide gauge data, which can appear as biases in the absolute validation even if there are not any true biases.

The ocean tide at the TG can be obtained from either harmonic analysis of the TG data or from a tide model. Harmonic analysis generally provides a much better prediction of the tide than a numerical model, particularly at the coast where local tidal effects can be difficult to model. Hence, in principle, we favour harmonic analysis over a model, but nevertheless we will compare the results based on both approaches and see how they differ.

When it is not possible to obtain ellipsoidal heights due to the unavailability of GPS data, the SLAs from the TG ( $\text{SLA\_Tg}$ ) will be obtained by removing the time mean from  $\text{SSH\_TG}$ .

In the Harvest region, TG data are hourly averages. This means that the maximum temporal separation between the in-situ and altimeter measurements, in the absence of data gaps, will be 30 min for the TGs. If gaps are present, we will still enforce a maximum separation of 30 min.

To obtain in-situ-altimetry comparison pairs, we will follow the approach that we have successfully used in previous validation activities (Calafat et al., 2017; Passaro et al., 2018; Bouffard et al., 2018). Briefly, this approach consists of assigning the altimetry data to distance bands of a certain width, and then averaging the altimetry records falling within each band. The corresponding in situ matching value is obtained by linearly interpolating the high-frequency observations to the time of the corresponding altimetry pass. Here, interpolating in time is preferred to simply selecting the closest point, particularly when comparing with TGs, since sea levels can vary significantly over a span of 30 minutes. Another point to consider is that TGs can be strongly influenced by vertical land motion. While here we focus on relatively short time scales at which the land contribution is expected to be small, we will still detrend both the altimetry and TG time series to avoid issues with potentially strong local land movements. Once matchup datasets are available, we will use standard quantitative statistical quantities to evaluate the quality of the new satellite altimeter data (bias, std, regression). These will be compared with similar quantities obtained with matchup datasets based on the content of the operational altimeter products.

## 2.3 Validation in the Gulf of Cadiz and Strait of Gibraltar regions (U Cadiz)

### 2.3.1 Study areas

The Gulf of Cadiz (Southwest Spain) has one of the main tributaries in Spain, the Guadalquivir River and the Doñana National Park wetlands on its right bank, close to its mouth on the Atlantic coast. Another tributary is the Tinto-Odiel System on the left of the Park. Past and present altimetry data have been validated in this area using *in situ* tide gauges deployed and managed by Puertos del Estado ([www.puertos.es](http://www.puertos.es)): Huelva station (in the mouth of the Tinto-Odiel System), Bonanza station (located in the estuary mouth of the Guadalquivir River), and Tarifa station (Strait of Gibraltar). The location of the study areas in the Iberian Peninsula is shown in Fig. 2.3.1.a. The location of the S3A/B tracks and the tide gauges (Huelva and Bonanza: Gulf of Cadiz) is given in Fig. 2.3.1.b; the same for the Strait of Gibraltar (Tarifa station and tracks) is in Fig. 2.3.1.c. The CryoSat-2 tracks are not shown here.

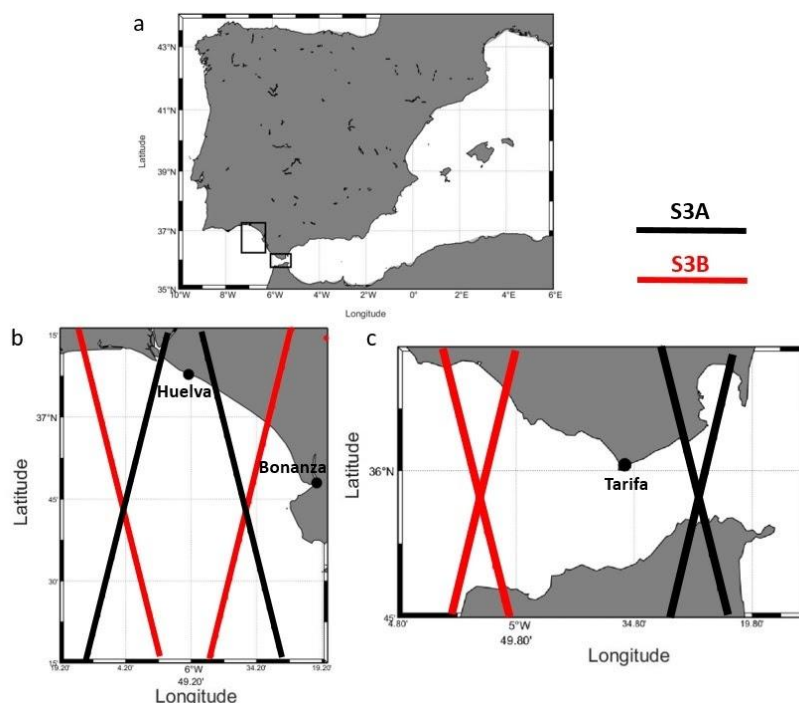


Figure 2.3.1. The Gulf of Cadiz and the Strait of Gibraltar in the Iberian Peninsula (Fig. 2.3.1.a). S3A/B tracks and TG stations in the Gulf of Cadiz (Huelva and Bonanza: Fig. 2.3.1.b) and in the Strait of Gibraltar (Tarifa: Fig.2.3.a.c).

The Huelva tide gauge station is located in the eastern shelf of the Gulf of Cadiz, Southwest of the Iberian Peninsula. Tides are mainly mesotidal, with amplitudes above 1 m. The Gulf of Cadiz surface circulation is characterized by a strong seasonality that is linked to the offshore circulation (Peliz et al., 2007). García-Lafuente et al. (2006) proposed the existence of a mesoscale cyclonic cell over the eastern continental shelf during spring-summer, its northern part being a warm coastal countercurrent (Stevenson, 1977; Relvas and Barton, 2002). This countercurrent is generally replaced by an eastward flowing current during autumn and winter (Criado-Aldeanueva et al., 2009). More recent studies (Garel et al., 2016) suggest that the onset of this countercurrent is a common feature over the year and does not show a seasonal behaviour. The Guadalquivir River also plays an important role in the eastern Gulf of Cadiz surface circulation. Sporadic but heavy freshwater discharges might contribute to the sea level at different time-scales as previously noted by Laiz et al. (2013) and Gómez-Enri et al. (2015; 2018).

The study area has also been used in the past for the validation of conventional pulse-limited and SAR-mode radar altimeter data near the shore. Gómez-Enri et al. (2012) and Laiz et al. (2013) used weekly gridded maps of SLA from AVISO (Archiving, Validation and Interpretation of Satellite data in Oceanography) to validate SLA time series at different time scales, finding high and significant correlations ( $r > 0.85$ ) with *in situ* tide gauge sea level data at monthly time scales. As mentioned before, Gómez-Enri et al. (2018) validated SLA time series from the CryoSat-2 SIRAL altimeter, in SAR mode, using the Huelva tide gauge. The authors analyzed along-track data with an along-track spatial resolution of 20 Hz, obtaining rmse of 6.4 – 8.5 cm in the 5 – 20 km segment respect to the coast. Furthermore, these values increased towards the coast, ranging from 8.5 to 29.3 cm in the 0 – 5 km segment. More recently, Aldarias et al. (2020) validated 2.3 years of Sentinel-3A 80-Hz sea level data (SARvatore-GPOD and SAMOSA+ (Dinardo et al., 2018) retracker) at Huelva TG station. They found accurate S3A sea level data (rmse < 10 cm) at the [2.5 – 20] km distances to the coast for the two tracks analyzed.

The Strait of Gibraltar is the choke point between the Atlantic Ocean and the Mediterranean Sea and controls the water exchanges between both water masses. The Strait of Gibraltar has been thoroughly described in the past from different points of view. Lacombe and Richez, 1982; Bryden and Kinder, 1991, analyzed the surface flux of Atlantic water toward the East being compensated by a western flux of Mediterranean deeper, saltier, and warmer water.

From an altimetric point of view, (Fukumori et al., 2007; Menemenlis et al., 2007) analyzed the sea level difference between the Atlantic Ocean and the Mediterranean Sea near the strait using Topex/Poseidon tracks. However, they only used along-track altimeter data at 1-Hz interval (about 6 km along the ground track) in regions deeper than 1000 m at distances greater than 150 km from the eastern and western sides of the Strait. They pointed out the lack of accurate altimeter data for shallower regions. More recently, Envisat RA-2 (18 Hz) and SARAL AltiKa (40 Hz) SLA were validated in the Strait using the Tarifa TG station obtaining rmse values between 12 – 14 cm (Envisat RA-2) and between 8 and 10 cm (SARAL AltiKa) within the first 30 km from the coast (Gómez-Enri et al., 2016). A few works are in progress on coastal applications using accurate altimeter data for a better knowledge of the hydrodynamic processes in the Strait (Gómez-Enri et al., 2019).

### 2.3.2 Times series of data

The HYDROCOASTAL altimeter-derived SLA time series will be estimated using Eq. (2.3.1):

$$SLA\_Retracker(n) = \text{Altitude} - \text{Range}(n) - (\text{Range Corrections} + \text{Geophysical Corrections}) - \text{MSS} \quad (2.3.1)$$

where  $n$  corresponds to the number of retracker used in coastal zones; *Orbit* (or *Altitude*) is the distance between the satellite's centre of mass and the reference surface (ellipsoid WGS84). *Range*( $n$ ) is the retracked distance between the instrument and the mean reflected surface obtained from the  $n$  retracker. *Range corrections* include the dry and wet tropospheric effect obtained from the University of Porto and ECMWF models, the ionospheric correction provided by the Global Ionospheric Maps (GIM) of the Jet Propulsion Laboratory, and the Dynamic Atmospheric Correction (DAC) provided by AVISO+/CNES. The *Geophysical corrections* include the ocean equilibrium tide, the ocean long period, the ocean load tide, the solid earth tide, and the pole tide. The *Mean Sea Surface* used will be surface available in the output product.

The Sea State Bias correction (SSB) will not be available in most of the retracker. In order to get a first approximation of this correction, a parametric approach will be made by estimating the best fit (in terms of the statistical approach selected) between  $SLA\_Retracker(n)$  and  $SLA\_TG$ , when SSB values ranging between 0% (no correction) and 10% of the SWH. Preliminary analysis made with S3A/B in Huelva and Tarifa (using the SARvatore-GPOD and SAMOSA+ (Dinardo et al, 2018) retracker) gave the results shown in Table 2.3.1. The percentage of SWH shown in the table (used as a first approximation of the SSB correction) gave the smaller rmse (see subsection 2.3.4 for details) between altimeter-derived SLA and ground-truth stations.

Table 2.3.1. Percentage of SWH to compute the SSB correction (as a first approximation) for the tracks analysed (S3A and B) at the two TG stations. Ocean-Land / Land-Ocean means the transition of the track segment.

Coasts	Huelva	Tarifa
S3A # (Ocean-Land)	4%	7%

S3A # (Land-Ocean)	4%	7%
S3B # (Ocean-Land)	5%	6%
S3B # (Land-Ocean)	7%	8%

The TG time series will be built using the time of the closest measurements to the time of the altimeter data. The temporal difference between altimeter and TG data is below 2.5 min. The Sea Levels will be obtained following Eq. (2.3.2):

$$\text{SLA\_TG} = \text{Water Level} - \text{Tide Prediction} - \text{DAC} \quad (2.3.2)$$

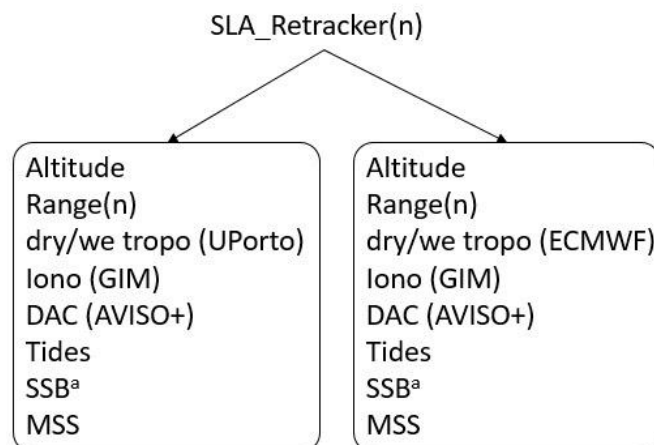
where *Water Level* is the sea level measurement; the Tide Prediction will be calculated from the tide gauges data with a classical harmonic analysis (Pawlowicz et al., 2002). *DAC* from AVISO+/CNES will be estimated by bilinear interpolation in space to the position of the TG station, and linear interpolation in time to the time of the instrument measurements.

### 2.3.3 Data screening

First, a data screening will be used to remove outliers: 1) the values outside the range: [-1.5, 1.5] m and 2) the values outside the median  $\pm 3 \sigma$  (standard deviation). In the second step, the temporal mean of the time series will be eliminated to obtain the anomalies.

### 2.3.4 Statistical approaches

The altimeter-derived time series (Fig. 2.3.2) will be validated with the SLA\_TG using two statistical parameters, namely, the *r* coefficient and the rmse, as in previous works (Fenoglio-Marc et al., 2015; Passaro et al., 2016; Dinardo et al., 2018; Gómez-Enri et al., 2018; Aldarias et al., 2020; among others). The validation will be focused on the along-track segments shown in Fig. 2.3.1 for S3A/B and the set of tracks for CryoSat-2, for the *n* retracker used in the coastal zones. The dry/wet tropospheric corrections from UPorto will be also assessed for each retracker (Fig. 2.3.2). The percentage of valid cycles in the track segments selected will be also computed.



n = 1 (2-step Analytical retracker (isardSAT))

n = 2 (Specialised SARin (Aresys))

n = 3 (MWaPP (DTU Space))

n = 4 (ICC-ER Empirical Retracker (ATK))

n = 5 (STARS Type (U Bonn))

n = 6 (ALES+ for SAR (TUM))

n = 7 (Specialised COastal OPERator for SAR - SCOOP-SAR (NOC))

<sup>a</sup> ALES+ for SAR is the only one providing the SSB correction

The SSB for the other retrackerers will be estimated analytically

Figure 2.3.2. Schematic representation of the altimeter-derived time series with the corrections and the selected retrackerers.

## 2.4 Influence of land proximity and angle of approach (SatOC/SKYMAT)

The performance of Sentinel-3 and CryoSat-2 SAR/SARin radar altimetry are examined by investigating their angle of approach towards the coastline. The performance of different re-trackerers is assessed in terms of noise and data loss for each satellite mission. A range of different coastline types are selected to represent various coastal physical features as well as having a wide variety of orientation angles approaching the coastline. Specifically, five selected regions reflecting different coastline types are considered: the Gulf of Cádiz, German Bight and Baltic, a mixture of relatively flat terrain, and Harvest and Straits of Gibraltar with higher cliffs.

The angle of approach to the coast is computed by calculating the separation angle between the direction of the satellite track and the direction of the gradient using the coastal proximity parameter (Cipollini, 2011). This method is described in more detail in the SCOOP Product Validation Report (PVR), D2.5, Section 4.4. In this study, the separation angle dependency is assessed at 15-degree divisions and binned at 1 km intervals as a function of distance to the coast in terms of data lost close to the coast (see example Figure 2.4.1). Here, the uncorrected sea surface height (USSH(n)) is calculated from Orbit minus Range(n), where n is the number of re-trackerers. No other corrections are applied. The noise is defined as successive differences of high frequency (20 Hz) USSH(n) observations along each of the tracks (Passaro et al. 2014).

This also allows us to calculate the USSH(n) noise as a function of the angle of approach to the coast for each re-tracker and satellite mission for comparisons. A baseline ESA product will be used as a standard in order to compare the re-trackers for noise and data loss. The analysis of the angle of approach associated with USSH noise and data loss to the coast will use the median filter, 25 and 75 percentiles as indicators for each re-tracker(n) per satellite mission per region. This methodology is repeated for the significant wave height (SWH(n)) observations.

#### 2.4.1 Data Screening/Filtering

A high resolution landmask will be created and applied to the satellite observations for each of the defined regions using the GMT software where the Global Self-consistent, Hierarchical, High-resolution Shorelines (GSHHS) dataset is used. Any USSH(n) values outside the median  $\pm 3 \sigma$  (standard deviation) will be removed. The misfit parameter will also be applied.

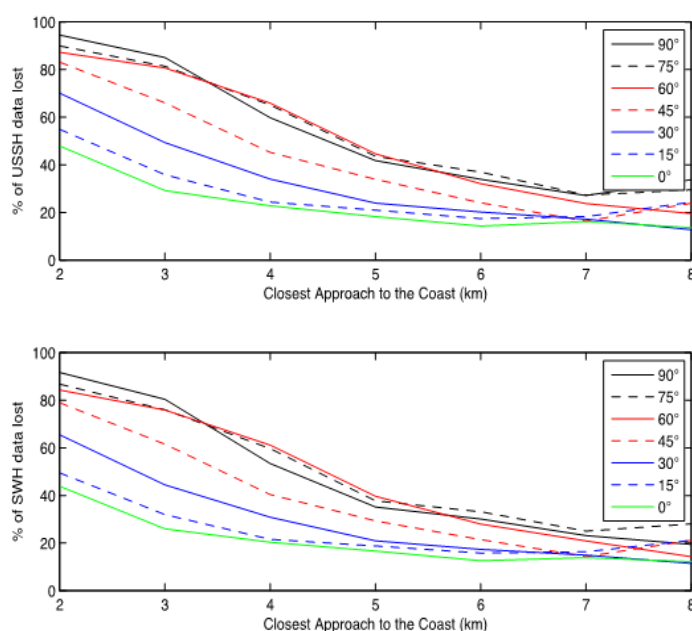


Figure 2.4.1. The percentage of the CryoSat-2 SAR Phase 2 data rejected when applying a misfit threshold of 3 from USSH and SWH parameter fields as a function of the angle of approach and distance to the coastline for the North East Atlantic region for 2012 to 2013 where 0° and 90° represents normal and parallel to the coast, respectively (SCOOP PVR, D2.5, Section 4.4)

## 3 Validation of the Test Datasets in different Inland Water Scenarios

In this section, we describe the activities that will be carried out to validate the Test Dataset Geophysical parameters against other satellites and in situ data, in different Inland Water Scenarios (e.g. low lands, hilly areas/valleys, man-made structures, estuaries).

These validation activities include the analysis of the influence of land proximity and ground-track orientation on SAR/SARin, analyses and exploitation of SAR/SARin stack data, the analyses of the different algorithms proposed to produce the final datasets of water level (L3) and river discharge (L4) and validation against gauging data.

### 3.1 Validation on the Rhine and Elbe rivers (U Bonn)

Validation activities focus on the Rhine and the Elbe rivers. The two regions are of interest for validation because of the large network of fiducial reference measurements available through the German national agencies (BfG, BKG). The location of the *in-situ* measurements is shown in Figures 3.1.1 for the Elbe Estuary and 3.1.2 for the river Rhine. Stations from the Netherlands (Rijkswaterstaat) will be considered for the River Rhine. A set of in-situ stations near to the altimeter virtual stations will be selected.

Water level time series derived by retracking will be compared to a set of external water level time series in order to assess their accuracy and to evaluate the impact of the new processing techniques. As quality indicators, metrics based on correlation and root mean square errors (RMSE) will be used. Virtual pass defines a virtual point and a polygon for each in-situ station. The altimeter measurements falling inside the polygon within a chosen distance from the virtual point are considered and screened out in the post-processing in case the moving standard deviation between three consecutive measurements is higher than 20 cm, see Dinardo (2020). The error assigned to the averaged altimeter height is the standard deviation of the averaged data, or the standard deviation read from the data products, if only one measurement is used.

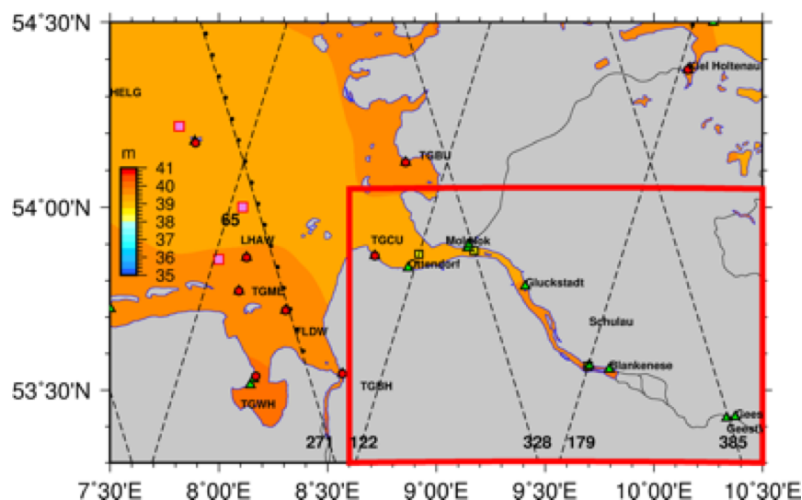


Figure 3.1.1. Elbe Estuary with in-situ stations and Sentinel-3A ground tracks

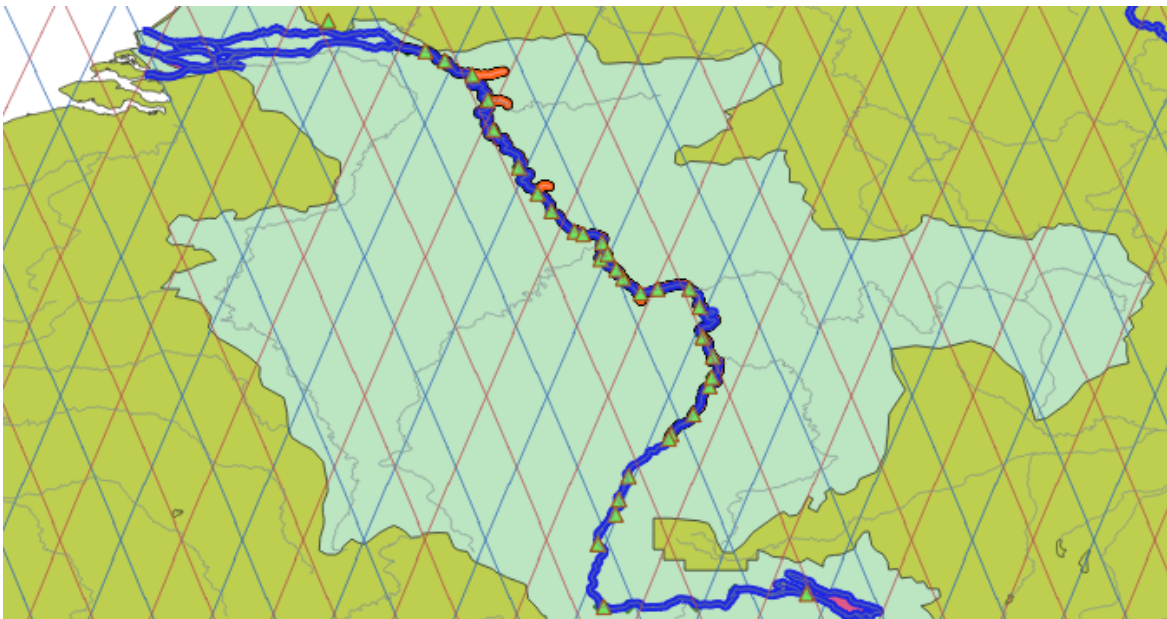


Figure 3.1.2. River Rhine with level gauge location (green triangle) and Sentinel-3A/3B (red/blue) tracks.

## 3.2 Validation of Water Level Time Series (DGFI/TUM)

In order to perform an independent assessment of inland water level time series derived from the different dataset providers, an inter-comparison as well as a validation in different globally distributed sites will be performed (by an institution not providing inland water level time series itself).

The HYDROCOASTAL inland water level time series (L3 data) will be compared to each other and to a set of external water level time series in order to assess their accuracy and to evaluate the impact of the new processing techniques. Moreover, the impact of different tropospheric corrections (standard and provided within this project) will be assessed. As quality indicators, we will use correlation, root mean square errors (RMSE), Nash-Sutcliffe-Efficiency (NSE), as well as offset analyses.

The external data sources used for comparison will be the following:

- in situ gauging data from different sources;
- Altimetry-derived water level time series as provided by DAHITI (<https://dahiti.dgfi.tum.de>; Schwatke et al., 2015). Depending on the availability of data, single-mission time series from Sentinel-3 as well as from other missions will be used. In addition, in case of larger lakes multi-mission time series are used;
- Lake level time series derived from surface area time series based on optical images (Schwatke et al., 2019) combined with (sparse) stage data following a hypsometry approach (e.g. Busker et al., 2019, Schwatke et al., 2020).

The validation will be performed on a set of different inland water bodies (rivers, lakes, and reservoirs) of different sizes and characteristics, globally distributed all over the continents. This will provide an overview on the quality of the new time series depending on target characteristics. Moreover, the impact of dedicated SAR processing (developed within HYDROCOASTAL) will be visible through the direct comparison with

Sentinel-3 DAHITI time series, which are treated in DAHITI just like classical LRM missions (i.e., based on standard retracking (with empirical ITR retracker) of multi-looked L1b waveforms).

### 3.3 WFRWF approach, influence of ground-track orientation and water fraction (ATK)

Land proximity and ground-track orientation are acceptable approaches in simple coastal cases (not in fjords, not in the case of small islands, small rivers, etc.). It has been noticed that these concepts provide both a degraded and an ambiguous representation of the altimeter footprint content, which is therefore inappropriate in most inland water cases (especially flooded plains). Instead, an analysis of the Water Content in the Footprint based on water masks will better correlate to the geophysics of the scene, and be more predictive and easier to handle. Such work has been initially developed in the frame of the SHAPE project (Fabry et al. 2015, 2016), cf. Fig. 3.3.1

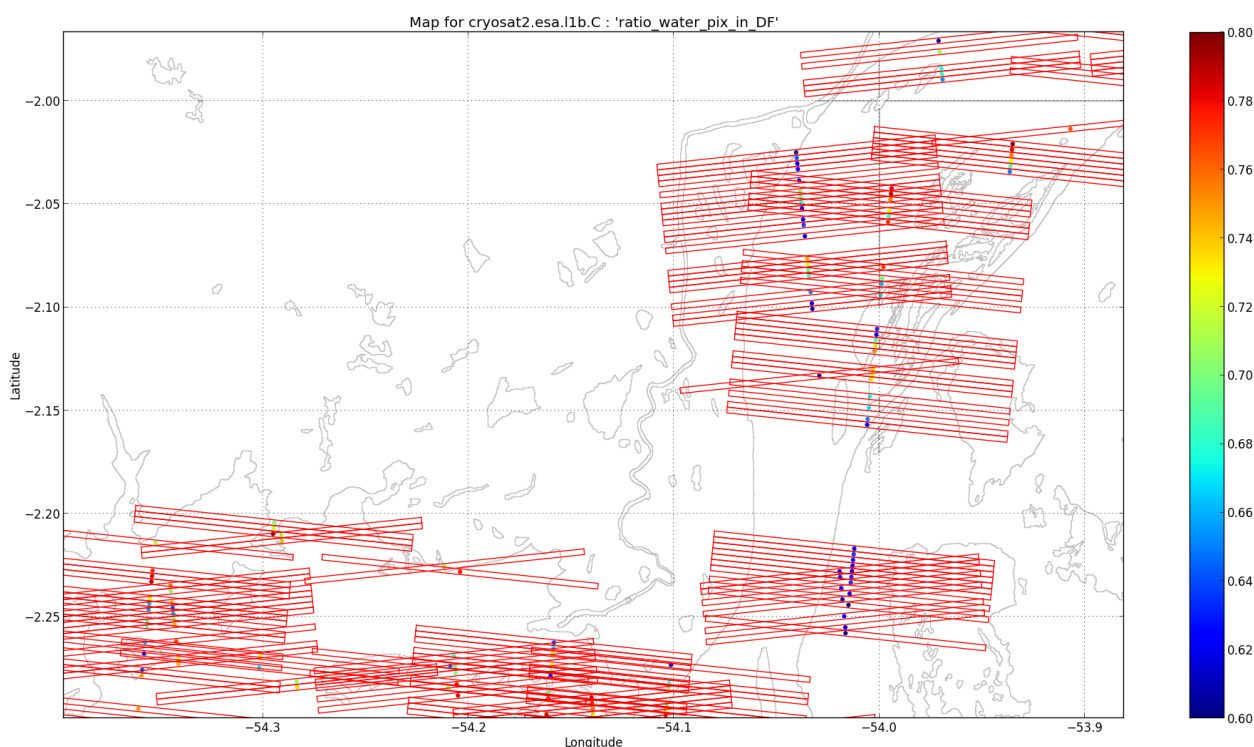


Figure 3.3.1. CryoSat-2 Baseline-C, Beam-Doppler limited footprints (20Hz records) over the Amazon downstream together with SWBD water masks on background and a central dot whose color indicates the water fraction (WFR) in each footprint (for the 60-80% interval here). (Extracted from Fabry et al., 2016, ATK.)

Currently (and in the illustration above) a coarse method is used to determine the Beam-Doppler limited footprint extent. The footprints are computed, at each record, from the longitude, latitude, tracker range, satellite altitude and velocity found in CryoSat-2 L1B files and system parameters (3dB antenna beam-width, burst PRF). As depicted in the figure above, the Beam-Doppler limited footprints are derived from several points along the beam limits in the local Earth-tangential plane (ENU: East North-Up). This makes

it possible to compute, for each footprint, the footprint area (FA) as well as the water area (WA) at the intersection with the water masks. We then define the water fraction as:

$$WFR = WA / FA. \text{ (Eq.3.3.1)}$$

The footprint size relates to the satellite velocity  $V_{sat}$ , its range to ground  $h$ , the central wavelength  $\lambda$ , and the burst  $PRF$ :

$$\Delta x = h \cdot \frac{\lambda}{2V_{sat}} \cdot \frac{PRF}{64} \text{ (Eq.3.3.2)}$$

An approximation of the across-track beam size  $D$  is:

$$D = h \cdot \tan\left(\theta_B + \frac{v}{2}\right) - h \cdot \tan\left(\theta_B - \frac{v}{2}\right) \text{ (Eq.3.3.3)}$$

where  $\theta_B$  is the 3dB across-track antenna aperture (roughly 1.2 deg) and  $v$  is the boresight angle (0 degree as the attitude angles have not been considered in this early version of the footprint computation module).

A finer method will probably be available for this project. This method fully accounts for the available attitude angles provided in the products. It consists in projecting the antenna boresight to its “exact” location at the surface (tracker range related) of the ellipsoidal Earth (WGS84). The along-track limits are then determined in the Earth-tangential plane (ENU: East North-Up) centered on this “exact” footprint centre using Eq. 3.3.2 while the across-track are now obtained from projecting the antenna across-track aperture to the ellipsoidal Earth. Improved WFR are expected upon the condition of using an up to date water mask.

## 3.4 Validation over the Amazon Basin (AHL)

Part of the TDS validation will be implemented over the Amazon basin for tens of virtual stations. This process leads to statistically significant results because of the large number of locations and measurements that can be validated.

Ideally speaking, gauging stations with vertical spirit leveling will be involved. In this case, quality indicators will include RMSE and mean error. However, for stations without trusted vertical spirit leveling RMSE and mean error will not be computed and the validation will be limited to Standard Deviation (relative validation). Other quality indicators, not related to vertical measurement, are the Sampling Loss Rate (SLR, %) and effective revisit period (in days). For L3 RWL time series, SLR indicates the ratio of lost measurements w.r.t. the nominal number of measurements (=1 per overflight).

The absolute vertical spirit leveling is available for almost one hundred of gauging stations (Kosuth et al., 2006), some other gauging stations might be used without spirit leveling. Figure 3.4.1 provides an overview of the leveled gauging data available vs. satellite coverage (CryoSat-2 mode masks and Sentinel-3A tracks).

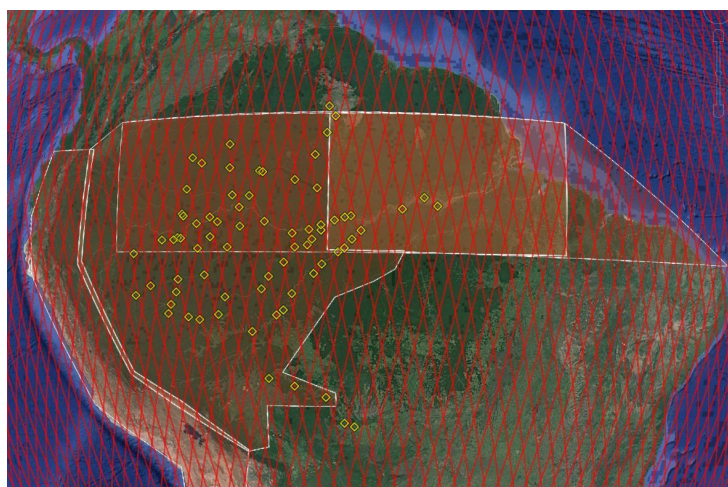


Figure 3.4.1. Map for TDS Validation of CryoSat-2 SARM & SARINM and Sentinel-3 SARM data against in situ gauging data over the Amazon basin. The Polygons represent the various CryoSat-2 SARM and SARIN Mode masks, red lines are Sentinel-3A tracks and yellow diamonds are the location of ANA gauging stations with absolute spirit leveling (96 stations), several hundreds of unleveled stations also exist and can be used to perform relative validation (i.e., no absolute bias computed).

In situ data availability over the Amazon basin is very good, however not always complete, but sometimes erroneous. The database that will be used is based on ANA data with some corrections applied to fix known errors (e.g., arbitrary shifts by 1m). Data are available within a delay ranging from 1 to 12 months (typically 6 months) depending on the gauging station. As a consequence, it is likely that too recent data will be eligible for validation.

### 3.5 Validation against in situ data for Amur, Yangtze and Zambezi (DTU)

The test dataset water surface elevation (WSE) will be validated against in-situ station observations for three continental-scale river systems, the Amur, the Yangtze and the Zambezi. In all 3 basins, previous studies have evaluated availability and performance of CryoSat-2 and Sentinel-3 water surface elevation (Jiang et al., 2017, Jiang et al., 2019, Jiang et al., 2020, Kittel et al., 2020). The test dataset WSE will be validated by calculating standard performance statistics for the different WSE datasets, including root mean squared error, correlation coefficient, mean absolute error and mean error. Table 3.5.1 lists stations in the Amur/Songhua system, available data types and data periods. Figure 3.5.1 shows a corresponding map.

Table 3.5.1. Available in-situ validation stations in the Amur

Station Name	Data type (WL=water level, Q=discharge)	In-situ data availability period
Harbin	WL + Q	2007-2014
Jiamusi	WL + Q	2007-2014
Yilan	WL + Q	2007-2014
Tonghe	WL + Q	2007-2014

Luobei	WL	2010-2012
Jiayin	WL	2010-2012
Fuyuan	WL	2010-2012



Figure 3.5.1. Available in-situ stations in the Amur-Songhua

Table 3.5.2 lists the stations in the Yangtze system, available data types and data periods. Figure 3.5.2 shows a corresponding map.

Table 3.5.2. Available in-situ validation stations in the Yangtze

Station Name	Data type (WL=water level, Q=discharge)	In-situ data availability period
Zhimenda	WL + Q	2016-19
Gangtuo3	WL + Q	2016-19
Shigu	WL + Q	2016-19
Panzhihua2	WL + Q	2016-19
Longjie3	WL	2016-19
Huatan	WL	2016-19

Yibin	WL	2016-19
Lizhuang	WL	2016-19
Luzhou3	WL	2016-19
Hejiang	WL	2016-19
Zhutuo3	WL + Q	2016-19
Cuntan	WL + Q	2016-19
Changshou2	WL	2016-19
Qingxichang3	WL	2016-19
Zhongxian	WL	2016-19
Wanxian2	WL	2016-19
Fengjie	WL	2016-19
Wushan	WL	2016-19
Badong3	WL	2016-19
Maoping2	WL	2016-19
Sandouping2	WL	2016-19
Huanglingmiao	WL + Q	2016-19
Yicang	WL + Q	2016-19
Zhicheng	WL + Q	2016-19
Majjadian	WL	2010-14,16-19
Chenjiawa	WL	2016-19
Shashi	WL + Q	2016-19
Haoxue	WL	2016-19
Xinchang2	WL	2016-19
Shishou	WL	2016-19
Tiaoxiankou	WL	2016-19
Jianli	WL + Q	2016-19
Luoshan	WL + Q	2010-14,16-19
Hankou	WL	2010-14,16-19
Huangshigang	WL	2016-19

Matouzhen	WL	2010-14,16-19
Jiujiang	WL	2010-14,16-19
Anqing	WL	2010-14,16-19
Datong	WL + Q	2010-14,16-19

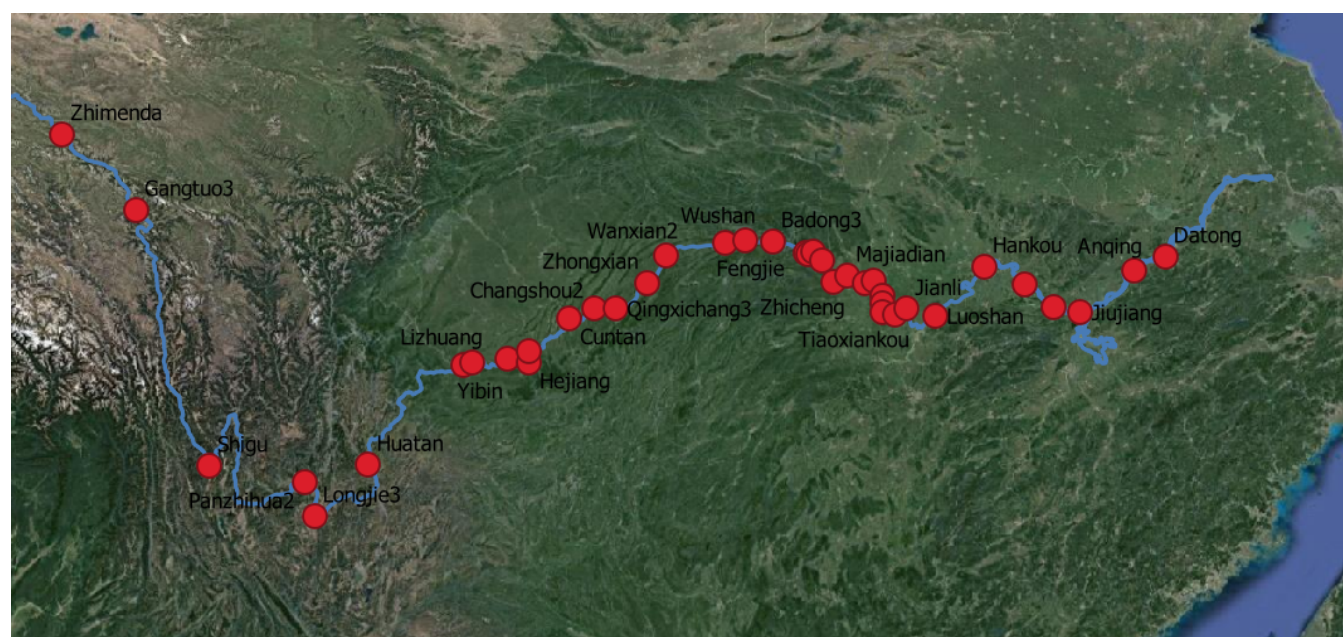


Figure 3.5.2. Available in-situ stations in the Yangtze

Table 3.5.3 lists stations in the Zambezi system, available data types and data periods. Figure 3.5.3 shows a corresponding map.

Table 3.5.3. Available in-situ validation stations in the Zambezi

Station Name	Data type (WL=water level, Q=discharge)	In-situ data availability period
Chavuma	WL + Q	2015-present
Watopa	WL + Q	2017-present
Lukulu	WL	2017-present
Kalabo	WL + Q	2017-present
Matongo Platform	WL	1956-present
Senanga	WL	1970-present
Ngonye Falls	WL + Q	2005-present

Sesheke	WL	1960-present
Nanas Farm	WL + Q	2013-present
Victoria Falls	WL + Q	1924-present
Kalomo	WL + Q	2006-present
Gwayi	WL + Q	1999-present
Ume	WL + Q	2008-present
Sanyati	WL + Q	2017-present

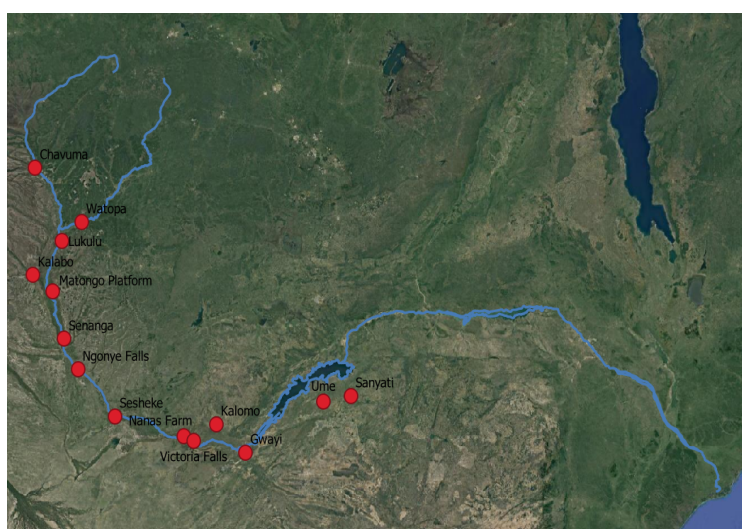


Figure 3.5.3. Available in-situ stations in the Zambezi

## 3.6 Validation against in situ data for Ob and Rhine Rivers (NUIM)

The altimetry-derived water (L3) and river discharge (L4) products will be validated against in situ observations of water level and discharge on one large Arctic River (the Ob) and one middle-size temporal climate river (the Rhine). In situ observations for the water level for the Ob River are available at Salekhard station for 2009-2020, while the discharge will be reconstructed using equations developed in Kouraev et al. (2004) and Zakharova et al. (2020) and based on information provided by Russian Hydrometeorological Service for earlier years. Special attention will be paid for the accuracy of the retrievals during ice season.

In situ observations of the water level for the Rhine River are available from automatic gauging stations located within the German territory. Several locations will be selected for validation of the water level retrievals to address an effect of the fluvial morphology (Fig. 3.6.1 (a)). The in-situ measurements are of 15-min frequency allowing for evaluation of effect of sub-daily level variability during the flood rise.

The river discharge will be calculated by three methods (rating curves, Bjerklie equation and Manning equation) and the accuracy of each method will be evaluated against in situ observations at annual scale and for a specific hydrological phase using common statistics:

- root mean square error (RMSE);
- correlation coefficient;
- bias.

To address the problem of the satellite sampling frequency and accuracy of altimetric freshwater fluxes estimates, monthly and annual water flow will be calculated from the altimetric retrievals. These values will be compared with similar quantities derived from daily in situ data.

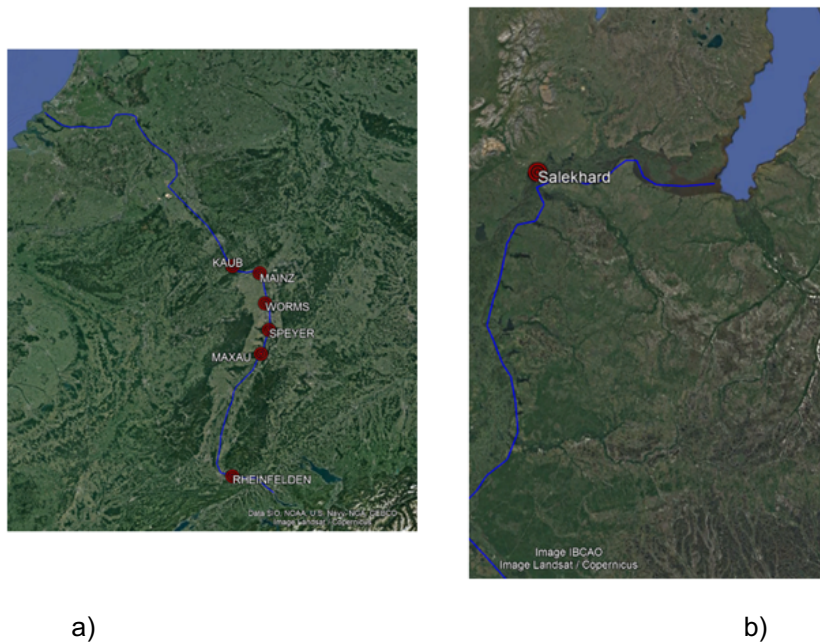


Figure 3.6.1 Location of discharge gauging stations on the Rhine (a) and Ob (b) Rivers.

### 3.7 Validation against in situ data for Po and Mississippi Rivers (CNR-IRPI)

The altimetry-derived water level (L3 product) and the simulated river discharge (L4 product) validation will be performed through the comparison of the products with in situ observations recorded at specific gauged stations. Specifically, thanks to the numerous gauged stations dislocated along the two selected rivers, Po and Mississippi, the validation procedure will be applied to sites not used for developing and implementing the algorithm for the river discharge estimation based on the merging between altimetry and imaging sensor. In such a way, an independent dataset of sites, not used in the previous steps, will be tested to ensure the quality of the algorithm.

The validation will be carried out at different scales, daily and monthly, and through both a direct comparison of temporal series and the duration-curve, that shows the percentage of time that flow in a stream (or water level) is likely to equal or exceed some specified values of interest.

Several metrics will be produced for water level and river discharge validation, considering in situ measurements. For the water levels, the following performance metrics will be produced:

- coefficient of correlation, to quantify the temporal agreement between in situ and satellite water level;
- root mean square error, to quantify the difference in magnitude between in situ and satellite water level;
- mean and standard deviation of the error to identify the statistical metrics.

The metrics will be evaluated in terms of relative heights to avoid influence of difference in datum (often unknown for the in situ measurements) or the distance between the virtual station and the gauged station. The relative heights will be computed by removing the long-term mean of both the temporal series.

For the river discharge, the above water level metrics will be used, along with:

- Nash-Sutcliffe efficiency index, a measure of goodness-of-fit with respect to the observed mean;
- the Kling-Gupta efficiency index, that provides direct assessment of four aspects of discharge time series, namely shape, timing, water balance and variability.

## 4 Validation of new DTC and WTC over CZ and IW regions (UPorto)

This section describes the set of procedures conducted by UPorto to assess the Dry Tropospheric Correction (DTC) and the Wet Tropospheric Correction (WTC) developed in WP2200 of the HYDROCOASTAL project.

This refers to the assessment performed by UPorto in the three selected test areas (Caspian Sea, Danube River and Java Sea). Additional independent validation of the corrections shall also be performed by other partners (in WP2500) in all test areas.

As the corrections are computed using an integrated approach, i.e., continuous corrections over all surface types (including ocean, coastal and inland water regions), a single validation plan is proposed.

Analyses will be performed both globally (for all test areas) and separately for the three selected areas: Caspian Sea, Danube River and Java Sea

### 4.1 Validation of the WTC

In this task, well established methodologies for the assessment of WTC datasets (Fernandes and Lázaro, 2016, 2018) will be adopted in the validation of the new WTC, namely:

- a) Comparison with the MWR-derived WTC present in products (only for S3) – for coastal regions and large lakes (Caspian and Java Seas).
- b) Comparison with the WTC from the ECMWF operational model – for all regions.
- c) Comparison with independent WTC from MWR on board the reference missions and from imaging sensors such as the Global Precipitation Measurement (GPM) Microwave Imager (GMI) - over coastal regions and large lakes (Caspian and Java Seas).
- d) Comparison with GNSS-derived WTC – this will provide information mainly about algorithm performance in the coastal regions and over IW regions with abundant number of GNSS stations.
- e) Sea/water level anomaly variance analysis, along track, at crossovers, function of distance from coast or from lake-border, and function of latitude.
- f) Error analysis based on the formal error, an additional output of the GPD+ algorithm.

### 4.2 Validation of the DTC

Since most errors associated with the DTC are systematic, validation diagnostics such as water level variance analysis are not appropriate. The following analysis shall be performed:

- a) Along-track analysis of DTC and water level profiles, inspecting unexpected behaviour of the correction, present in some current products
- b) Comparison with DTC present in products and with DTC derived from in situ pressure data, where available.

## 5 References

Aldarias, A., Gómez-Enri, J., Laiz, I., Tejedor, B., Vignudelli, S., Cipollini, P. Validation of Sentinel-3A SRAL Coastal Sea Level Data at High Posting Rate: 80 Hz. *IEEE Transactions on Geoscience and Remote Sensing*, 58, 6, 3809-3821. doi: 10.1109/TGRS.2019.2957649. 2020.

Bouffard, J., Naeije, M., Banks, C.J., Calafat, F.M., Cipollini, P., Snaith, H.M., Webb, E., Hall, A., Mannan, R., Féménias, P. and Parrinello, T., 2018. CryoSat ocean product quality status and future evolution. *Advances in Space Research*, 62(6), pp.1549-1563.

Bryden, H. L. Kinder, T. H. Steady two-layer exchange through the Strait of Gibraltar, *Deep-Sea Research.*, doi: 10.1016/S0198-0149(12)80020-3. 1991.

Busker T., de Roo A., Gelati E., Schwatke C., Adamovic M., Bisselink B., Pekel J.-F., Cottam A.: A global lake and reservoir volume analysis using a surface water dataset and satellite altimetry. *Hydrology and Earth System Sciences*, 23(2), 669-690, 10.5194/hess-23-669-2019, 2019

Calafat, F. M., P. Cipollini, J. Bouffard, H. Snaith, P. Féménias. Evaluation of new CryoSat-2 products over the ocean, *Remote Sens. Environ.*, 191, 131-144, 2017.

Cipollini, P. (2011). A new parameter to facilitate screening of coastal altimetry data and corrections. Presented at the 5th Coastal Altimetry Workshop, San Diego, USA available from [http://www.coastalt.eu/sites/default/files/sandiegoworkshop11/poster/P08\\_Cipollini\\_Castal\\_Proximity.pdf](http://www.coastalt.eu/sites/default/files/sandiegoworkshop11/poster/P08_Cipollini_Castal_Proximity.pdf)

Criado-Aldeanueva, F., García-Lafuente, J., Navarro, G., Ruiz, J. Seasonal and interannual variability of the surface circulation in the eastern Gulf of Cadiz (SW Iberia). *Journal of Geophysical Research: Oceans*, 114(C1). doi: 10.1029/2008JC005069. 2009.

Dinardo S., Fenoglio-Marc L., Buchhaupt C., Becker M., Scharro R., Fernandez J. Benveniste J. (2018). CryoSat-2 performance along the German coasts, *AdSR special Issue CryoSat-2*, <https://doi.org/10.1016/j.asr.2017.12.018>

Dinardo S., Fenoglio L., M. Becker; R. Scharroo; M. J. Fernandes; J. Staneva; S. Grayek; J. Benveniste (2020), A RIP-based SAR Retracker and its application in North East Atlantic with Sentinel-3, *Advances in Space Research* (2020), doi: <https://doi.org/10.1016/j.asr.2020.06.004>

Dinardo, S., 2020. Techniques and applications for Satellite SAR Altimetry over water, land and ice. PhD Dissertation Thesis. 56, Darmstadt, Germany, Technische Universität Darmstadt, ISBN 978-3-935631-45-7. <https://doi.org/10.25534/tuprints-00011343>.

Fabry P., Bercher N., Roca M., Martinez B., Fernandes J., Lázaro C., Gustafsson D., Arheimer B., Ambrózio A, Restano M, Benveniste J. (2016). "A step towards the characterization of SAR Mode Altimetry Data over Inland Waters – SHAPE Project". In "New era of altimetry, new challenges", Ocean Surface Topography Science Team meeting (OSTST), 31 Oct – 4 Nov 2016, La Rochelle, France

Fabry, P. and Bercher, N. (2015). "Characterization of SAR Mode Altimetry over Inland Water". In *Proceedings of the Sentinel-3 for Science Workshop*, 2-6 June, Venice, Italy

Fenoglio-Marc, L., Dinardo, S., Scharroo, R., Roland, A., Dutour, M., Lucas, B., Becker, M., Benveniste, J., Weiss, R. (2015): The German Bight: a validation of CryoSat-2 altimeter data in SAR mode, *Adv. Space Res.*, doi: 10.1016/j.asr.2015.02.014

---

Fenoglio-Marc, L., Dinardo, S., Buchhaupt, C., Scharroo, R., Becker, M., and Benveniste, J. (2019). Calibrating the SAR Sea Surface Heights of CryoSat-2 and Sentinel-3 along the German coasts. In Proceedings of International Association of Geodesy Symposia

Fenoglio L., S. Dinardo, B. Uebbing, C. Buchhaupt, M. Gärtner, J. Staneva, M. Becker, A. Klose, J. Kusche, M. Becker. Investigating improved coastal Sea Level Change from Delay Doppler Altimetry in the North-Eastern Atlantic, *Adv. Space Res.*, under review

Fernandes, M. J., Lázaro, C. (2016). GPD+ Wet Tropospheric Corrections for CryoSat-2 and GFO Altimetry Missions. *Remote Sensing*, 8(10), 851. doi:10.3390/rs8100851

Fernandes, M. J., Lázaro, C. (2018). Independent assessment of Sentinel-3A wet tropospheric correction over the open and coastal ocean. (2018) *Remote Sensing*, 10(3), 484. doi:10.3390/rs10030484

Fukumori, I., Menemenlis, D. Lee, T. A near-uniform basin-wide sea level fluctuation of the Mediterranean Sea. *Journal of Physical Oceanography*. doi: 10.1175/JPO3016.1. 2007.

García-Lafuente, J., Delgado, J., Criado-Aldeanueva, F., Bruno, M., del Río, J., Vargas, J. M. Water mass circulation on the continental shelf of the Gulf of Cadiz. *Deep Sea Research Part II: Topical Studies in Oceanography*, 53(11-13), 1182-1197. doi: 10.1016/j.dsr2.2006.04.011. 2006.

Garel, E., Laiz, I., Drago, T., Relvas, P. Characterisation of coastal counter-currents on the inner shelf of the Gulf of Cadiz. *Journal of Marine Systems*, 155, 19-34. doi: 10.1016/j.jmarsys.2015.11.001. 2016.

Gómez-Enri, J., Aboitiz, A., Tejedor, B., Villares, P. Seasonal and interannual variability in the Gulf of Cadiz: Validation of gridded altimeter products. *Estuarine, Coastal and Shelf Science* 96, 114-121. doi: 10.1016/j.ecss.2011.10.013. 2012.

Gómez-Enri, J., Escudier, R., Pascual, A., Mañanes, R. Heavy Guadalquivir River discharge detection with satellite altimetry: The case of the Eastern continental shelf of the Gulf of Cadiz (Iberian Peninsula). *Advances in Space Research*. DOI: 10.1016/j.asr.2014.12.039. 2015.

Gómez-Enri, J., P. Cipollini, M. Passaro, S. Vignudelli, B. Tejedor, J. Coca. Coastal altimetry products in the Strait of Gibraltar. *IEEE Transactions on Geoscience and Remote Sensing*. 54, 5455-5466. doi: 10.1109/TGRS.2016.2565472. 2016.

Gómez-Enri, J., Vignudelli, S., Cipollini, P., Coca, J., González, C.J. Validation of CryoSat-2 SIRAL sea level data in the eastern continental shelf of the Gulf of Cadiz (Spain). *Advances in Space Research*. doi: 10.1016/j.asr.2017.10.042. 2018.

Gómez-Enri, J., González, C.J. Passaro, M., Vignudelli, S. Álvarez, O., Cipollini, P., Mañanes, R., Bruno, M., López-Carmona, M.P., Izquierdo, A. Wind-induced cross-strait sea level variability in the Strait of Gibraltar from coastal altimetry and in-situ measurements. *Remote Sensing of Environment*, 221, 596-608. doi: 10.1016/j.rse.2018.11.042. 2019.

Jiang, L., Nielsen, K., Andersen, O. B., Bauer-Gottwein, P. CryoSat-2 radar altimetry for monitoring freshwater resources of China. *Remote Sensing of Environment*, 200, 125-139. doi: 10.1016/j.rse.2017.08.015. 2017

Jiang, L., Madsen, H., Bauer-Gottwein, P. Simultaneous calibration of multiple hydrodynamic model parameters using satellite altimetry observations of water surface elevation in the Songhua River. *Remote Sensing of Environment*, 225, 229-247. doi: 10.1016/j.rse.2019.03.014. 2019

Jiang, L., Nielsen, K., Dinardo, S., Andersen, O. B., Bauer-Gottwein, P. Evaluation of Sentinel-3 SRAL SAR altimetry over Chinese rivers. *Remote Sensing of Environment*, 237, 111546. doi: 10.1016/j.rse.2019.111546. 2020

Kittel, C. M. M., Jiang, L., Tøttrup, C., Bauer-Gottwein P. Sentinel-3 radar altimetry for river monitoring – a catchment-scale evaluation of satellite water surface elevation from Sentinel-3A and Sentinel-3B. *Hydrol. Earth Syst. Sci. Discuss.*, <https://doi.org/10.5194/hess-2020-165>, 2020. Preprint under review for HESS

Kosuth P., Blitzkow D., Cochonneau G. (2006). "Establishment of an altimetric reference network over the Amazon basin using satellite radar altimetry (Topex/Poseidon)", in the proceedings of the "15 years of progress in radar altimetry" Symposium, Venice, Italy.

Kouraev A.V., Zakharova E.A., Samain O., Mognard-Campbell N., Cazenave A. "Ob' river discharge from TOPEX/Poseidon satellite altimetry data". *Remote Sensing of Environment*, 93, 2004, pp. 238-245

Lacombe, H. Richez, C. The regime in the Strait of Gibraltar. In *Hydrodynamics of Semi-Enclosed Seas*, Jacques C.J. Nihoul (ed.), ISBN: 978-0-444-42077-0, 13-73. 1982.

Laiz, I., Gómez-Enri, J., Tejedor, B., Aboitiz, A., Villares, P. Seasonal sea level variations in the gulf of Cadiz continental shelf from in-situ measurements and satellite altimetry. *Continental Shelf Research* 53, 77-88. doi: 10.1016/j.csr.2012.12.008. 2013.

Menemenlis, D. Fukumori, I. Lee, T. Atlantic to Mediterranean Sea Level Difference Driven by Winds near Gibraltar Strait. *Journal of Physical Oceanography*. doi: 10.1175/JPO3015.1. 2007.

Passaro, M., P. Cipollini, S. Vignudelli, G. Quartly, and H. Snaith, (2014) "ALES: A multi-mission subwaveform retracker for coastal and open ocean altimetry", *Remote Sensing of the Environment*, vol. 145, pp. 173-189, 2014.

Passaro, M., Dinardo, S., Quartly, G.D., Snaith, H.N., Benveniste, J., Cipollini, P., Lucas, B. Cross-calibrating ALES Envisat and CryoSat-2 Delay-Doppler: a coastal altimetry study in the Indonesian Seas. *Adv. Space Res.* 58, 289–303. doi: 10.1016/j.asr.2016.04.011. 2016.

Passaro M., Rose S.K., Andersen O.B., Boergens E., Calafat F.M., Dettmering D., Benveniste J.: ALES+: Adapting a homogenous ocean retracker for satellite altimetry to sea ice leads, coastal and inland waters. *Remote Sensing of Environment*, 211, 456-471, 10.1016/j.rse.2018.02.074, 2018.

Pawlowicz, R., Beardsley, B., & Lentz, S. Classical tidal harmonic analysis including error estimates in MATLAB using T\_TIDE. *Computers & Geosciences*, 28(8), 929-937. 2002.

Peliz, A., Dubert, J., Marchesiello, P., Teles-Machado, A. Surface circulation in the Gulf of Cadiz: Model and mean flow structure. *Journal of Geophysical Research-Oceans* 112. doi: 10.1029/2007JC004159. 2007

Relvas, P., Barton, E. D. Mesoscale patterns in the Cape Sao Vicente (Iberian peninsula) upwelling region. *Journal of Geophysical Research: Oceans*, 107(C10), 28-1. doi: 10.1029/2000JC000456. 2002.

Schwatke C., Dettmering D., Bosch W., Seitz F.: DAHITI – an innovative approach for estimating water level time series over inland waters using multi-mission satellite altimetry. *Hydrology and Earth System Sciences* 19(10): 4345-4364, 10.5194/hess-19-4345-2015, 2015

Schwatke C., Scherer D., Dettmering D.: Automated Extraction of Consistent Time-Variable Water Surfaces of Lakes and Reservoirs Based on Landsat and Sentinel-2. *Remote Sensing*, 11(9), 1010, 10.3390/rs11091010, 2019

Schwatke C., Dettmering D., Seitz F.: Volume Variations of Small Inland Water Bodies from a Combination of Satellite Altimetry and Optical Imagery. *Remote Sensing*, 12(10), 1606, 10.3390/rs12101606, 2020

Stevenson, R.E. Huelva Front and Malaga, Spain, Eddy chain as defined by satellite and oceanographic data. *Deutsche Hydrographische Zeitschrift* 30 (2), 51–53. doi: 10.1007/BF02226082. 1977.

Zakharova EA., Nielsen K., Kamenev G., Kouraev A., River discharge estimation from radar altimetry: Assessment of satellite performance, river scales and methods, *Journal of Hydrology*, 2020, 583, 124561.

# List of Acronyms

ACE2	Altimeter Corrected Elevations (vers. 2)	CryoSat-2	Altimetry satellite for the measurement of the polar ice caps and the ice thickness
AD	Applicable Documents	CRISTAL	Copernicus polaR Ice and Snow Topography ALtimeter
AGC	Automatic Gain Control	CRUCIAL	CRyosat-2 sUCcess over Inland wAter and Land
AH	Alti-Hydro	CSV	Coma Separated Values
AHP	Alti-Hydro Product(s)	CTOH	Centre de Topographie des Océans et de l'Hydrosphère (Centre of Topography of the Oceans and the Hydrosphere)
AI	Action Item	DAC	Dynamic Atmospheric Correction
AIM	Action Item Management (tool)	DAHITI	Database for Hydrological Time Series of Inland Waters
AltiKa	Altimeter in Ka band and bi-frequency radiometer instrument	DAO	Data Access Object
AMSR-E	Advanced Microwave Scanning Radiometer-Earth Observing System	DARD	Data Access Requirement Document
ANA	Agência Nacional de Águas (National Water Agency, Brazil)	DDM	Delay-Doppler Map
AoA	Angle of arrival	DDP	Delay-Doppler Processor
API	Application Programming Interface	DEM	Digital Elevation Model
AR	Acceptance Review	DGC	Doppler Ground Cell
ASAP	As Soon As Possible	DPM	Detailed Processing Model
ASCII	American Standard Code for Information Interchange	DPP	Data Procurement Plan
ATBD	Algorithm Technical Basis Document	DTC	Dry Tropospheric Correction
ATK	ALONG-TRACK S.A.S.	DTU	Danmarks Tekniske Universitet (Technical University of Denmark)
AVISO	Archivage, Validation et Interprétation des données des Satellites Océanographiques	DVT	Data Validation Table
BfG	German Federal Institute of Hydrology	ECMWF	European Centre for Medium-Range Weather Forecasts
BKG	German Federal Agency for Cartography and Geodesy	ECSS	European Cooperation for Space Standardisation
BSH	German Federal Maritime and Hydrographic Agency	EGM	Earth Gravitational Model
BIPR	Background Intellectual Property Right	ENVISAT	ENVIronment SATellite
CASH	Contribution de l'Altimétrie Spatiale à l'Hydrologie (Contribution of Space Altimetry to Hydrology)	EO	Earth Observation
CCN	Contract Change Notice	EOEP	Earth Observation Enveloppe Programme
CFI	Customer Furnished Item	EOLi	Earth Observation Link
CLASS	NOAA/Comprehensive Large Array-Data Stewardship System	EOLi-SA	EOLi-Stand Alone
CoG	Centre of Gravity	EPN	EUREF Permanent Network
CNES	Centre Nationales des Etudes Spatiales	ERA	Iterim ECMWF ReAnalysis
CPP	CryoSat-2 Processing Prototype (CNES)	ESA	European Space Agency
		EUREF IAG	Reference Frame Sub-Commission for Europe

FBR	Full Bit Rate	ISD	isardSAT
FFT	Fast Fourier Transform	ITR	Improved Threshold Retracker
FR	Final Review	ITRF	International Terrestrial Reference Frame
FTP	File Transfer Protocol	IRF	Impulse Response Function
FCUP	(from portuguese) “ <i>Faculdade de Ciências da Universidade</i> ”, Science faculty of the University of Porto	Jason-1	Altimetry satellite, T/P follow-on
GDAL	Geospatial Data Abstraction Library	Jason-2	Altimetry satellite, also known as the « Ocean Surface Topography Mission » (OSTM), Jason-1 follow-on
GDR, [I-,S-]	Geophysical Data Record, [Interim-, Scientific-]	Jason-3	Altimetry satellite, Jason-2 follow-on
GFZ	Deutsche GeoForschungsZentrum (German Research Centre for Geosciences)	Jason-CS	Jason Continuity of Service
GIM	Global Ionospheric Maps	KML	Keyhole Markup Language
GLOSS	Global Sea Level Observing System	KO	Kick Off
GNSS	Global Navigation Satellite System	L1A	Level-1A
GOCE	Gravity field and steady-state Ocean Circulation Explorer	L1B	Level-1B
GPD	GNSS-derived Path Delay	L1B-S, L1BS	Level-1B-S (aka, Stack data)
G-POD	Grid Processing on Demand	L2	Level-2
GPT2	Global Pressure and Temperature model (vers. 2)	L3	Level-3
GPP	Ground Processing Processor	L4	Level-4
GPS	Global Positioning System	LAGEOS	Laser Geodynamics Satellite
GRACE	Gravity Recovery And Climate Experiment	LEGOS	(french acr.) Laboratoire d'Études en Géophysique et Océanographie Spatiale (Laboratory for Studies in Geophysics and Spatial Oceanography)
GRDC	Global Runoff Data Centre	LOTUS	Preparing Land and Ocean Take Up from Sentinel-3
GRGS	Groupe de Recherche de Géodésie Spatiale (Space Geodesy Research Group)	LPS	Living Planet Symposium
GRLM	Global Reservoir and Lake Monitor	LRM	Low Resolution Mode
GSHHS	Global Self-consistent, Hierarchical, High-resolution Shorelines	LSE	Least Square Estimator
GTN-L	Global Terrestrial Network - Lakes	LWL	Lake Water Level
HDF-EOS	Hierarchical Data Format - Earth Observing System	LWS	Low Water Stage
HGT	A SRTM file format	MARS	Meteorological Archival and Retrieval System
HWS	High Water Stage	MDL	Minimum Description Length
HYCOS	Hycos Hydraulics & Control Systems	MMSE	Minimum Mean Square Error
HYPE	Hydrological Predictions for the Environment model	MNDWI	Modification of Normalised Difference Water Index
IAG	International Association of Geodesy	MoM	Minutes of Meeting
IDAN	Intensity-Driven Adaptive-Neighbourhood	MPC	Mission Performance Centre
IE	Individual Echoes	MRC	Mekong River Commission
IGS	International GNSS (Global Navigation Satellite Systems) Service	MTR	Mid Term Review
IM	Internal Meeting (e.g. not with the client)	MSS	Mean Square Slope
IODD	Input Output Data Document	MSS	Mean Sea Surface
IPF	Integrated Processing Facility	MWR	Microwave Radiometer
		NAVATT	Navigation and Attitude
		NDBC	US National Data Buoy Center
		NDVI	Normalised Difference Vegetation Index

NDWI	Normalised Difference Water Index	rmse	root mean square error
netCDF	Network Common Data Form	ROI	(geographical) Region(s) Of Interest
NOAA	National Oceanic and Atmospheric Administration	RP	Report Period (a month that is being reported into a Progress Report)
NR	New Requirement (w.r.t. the SoW)	RSS	Remote Sensing Systems
NRT	Near Real-Time	RWD	River Water Discharge
NWM	Numerical Weather Model	RWL	River Water Level
OCOG	Offset Centre of Gravity	SAMOSA	SAR Altimetry MOde Studies and Applications
OPC	One per Crossing	SARAL	In Indian "simple", in english "SATellite for ARgos and AltiKa.
OSTM	Ocean Surface Topography Mission (also known as Jason-2), is also the name of the satellites series T/P, Jason-1, Jason-2 and Jason-3	SARIn	SAR Interferometric (CryoSat-2/SIRAL mode)
OVS	Orbit State Vector	SAR	Synthetic Aperture Radar
PDF	Probability Density Function	SARvatore	SAR Versatile Altimetric Toolkit for Ocean Research & Exploitation
PEACHI	Prototype for Expertise on AltiKa for Coastal, Hydrology and Ice	SCOOP	SAR Altimetry Coastal & Open Ocean Performance
PEPS	Sentinel Product Exploitation Platform (CNES)	SDP	Software Development Plan
PISTACH	(french acr.) Prototype Innovant de Système de Traitement pour les Applications Cotières et l'Hydrologie	SEOM	Scientific Exploitation of Operational Missions
PLRM	Pseudo Low Rate Mode	SHAPE	Sentinel-3 Hydrologic Altimetry Prototype
PMP	Project Management Plan	SI-MWR	Scanning Imaging MWR
POCCD	Processing Options Configuration Control Document	SLA	Sea Level Anomaly
PR	Progress Report	SLR	Sampling Loss Rate
PRF	Pulse Repetition Frequency	SME	Small and Medium-sized Enterprise
PSD	Product Specification Document	SMHI	Swedish Meteorological and Hydrological Institute
PSMSL	Permanent Service for Mean Seal Level	SNAP	SeNtinel Application Platform
PTR	Point Target Response	SOA	State Of the Art
PVP	Product Validation Plan	SONEL	Système d'Obserbvations du Niveau des Eaux Littorales
PVR	Product Validation Report	SOW	Statement Of Work
PVS	Pseudo Virtual Station(s)	SPR	Software Problem Reporting
RADS	Radar Altimeter Database System	SPS	Sentinel-3 Surface Topography Mission System Performance Simulator
RB	Requirements Baseline (document)	SRAL	SAR Radar Altimeter
RCMC	Range Cell Migration Curve	SRTM	Shuttle Radar Topography Mission
RCS	Radar Cross Section	SSB	Sea State Bias
RD	Reference Document	SSH	Sea Surface Height
RDSAR	Reduced SAR (also known as Pseudo-LRM)	SSM/I/IS	Special Sensor Microwave Imager (SSM/I) Sounder
RF	Random Forest	SSO	Single Sign-On
RGB	Red, Green, Blue	Stack	Matrix of stacked Doppler beams
RID	Review Item Discrepancy	STD	Standard Deviation
RIP	Range Integrated Power (of the MLD) sometimes referred as Angular Power Response (APR)	STDD	Standard Deviation of Differences
RMS	Root Mean Square		

---

STM	Sentinel-3 Surface Topography Mission	USO	Ultra Stable Oscillator
SUM	Software User Manual	USSH	Uncorrected Sea Surface Height
SWBD	SRTM Water Body Data	UTC	Coordinated Universal Time
SWH	Significant Wave Height	UWM	Updated Water Mask
TAI	Temps Atomique International (International Atomic Time)	VS	Virtual Station(s)
TBC	To Be Confirmed	VH	Vertical-Horizontal polarisation
TBD	To Be Done	VV	Vertical-Vertical polarisation
TCWV	Total Column Water Vapour	WBS	Work Breakdown Structure
TDS	Test Data Set	WFR	Water Fraction Ratio
TMI	Tropical Rainfall Measuring Mission (TRMM) Microwave Imager	WFRWF	Water Fraction Ratio - Water content in Footprint
TN	Technical Note	WMO	World Meteorological Organization
T/P	Topex/Poseidon (altimetry satellite)	WP	Work Package(s)
TR	Technical Risk	w.r.t.	with respect to
UNESCO	United Nations Educational, Scientific and Cultural Organization	WTC	Wet Tropospheric Correction
URL	Uniform Resource Locator	XML	eXtensible Markup Language
USGS	United States Geological Survey	ZP	Zero Padding